Simulation and Analysis on Flow Field of Nozzle Position of Hydraulic Thruster Based on CFD

Xie Wujun, Zhang Derong, Wu Simeng, Pu Yangfeng

School of Mechatronic Engineering, Southwest Petroleum University, PR China, 610500

Abstracts: ***In this paper, the flow field characteristics of the nozzle of a hydraulic hydraulic thruster are analyzed by CFD method based on the design of the nozzle part of the hydraulic thruster. The analysis results show that the velocity vector map and the pressure cloud map of the flow field model gradually increase from the inlet to the nozzle, and then gradually decrease from the nozzle to the outlet. The erosion area is mainly located near the flow area of the nozzle. The maximum erosion speed is in the flow part of the nozzle. The pressure is gradually smaller from the inlet to the outlet. The pressure is gradually reduced from the inlet to the nozzle, and then the nozzle to the outlet is gradually increased, and the pressure of the nozzle is minimal; the flow velocity of the pipe is found to be change about 60~90m/s from exit to entrance. The mainstream fluid pressure increases gradually from inlet to outlet, and changes from about 25.5MPa~26.5MPa. The three-dimensional flow of the flow field near the nozzle of a hydraulic thruster under different velocity and pressure is simulated by CFD software, which provides a new basis for the design of the nozzle structure of the hydraulic thruster.***

Keywords: Hydraulic thruster; Flow field; CFD; Simulation

1. Introduction

Hydraulic thruster is generally used in drilling and workover operations of extended reach wells and horizontal wells to achieve rock breakage and clean bottom. The hydraulic pressurizer transforms the mud power into the axial thrust through the throttle effect, which can reduce the drillpressure fluctuation caused by the drill string meditation vibration and the interaction of the drill and rock, thus exerting a relatively constant drilling pressure to the bit, prolonging the bit life, reducing the fatigue failure of the drill and improving the drilling efficiency, which is a kind of high pressure mud. An energy conversion device that transforms pressure into broken rock. At present, scholars at home and abroad have studied the hydraulic pressurizer. Lin Yuanhua et al [1] designed a hydraulic pressurizer that can provide a constant and easy to control drilling pressure, which can be widely used in the oil field because it absorbs the percussion of the bit. Liu Jianmin et al [2] through the experimental results show that the use of hydraulic pressure device can provide smooth drilling pressure, reduce the axial vibration of drilling tools, reduce the fatigue failure of drilling tools, prolong the service life of the drill, and improve the speed of mechanical drilling. Liu Qinzhi et al [3] detailed the function, structure, characteristic technical parameters, use method and performance test of hydraulic pressurizer. The performance and reliability of the product meet the design requirements in the test of the bench performance. In the process of Tan Chunfei et al [4] continuous pipe drilling, it is difficult to apply the drill pressure of the bottom drill assembly without drill collar, and a calculation model of the axial thrust produced by the hydraulic pressurizer in series over the turbodrill is established. JOHN EM[5] puts forward that reducing the positive pressure and friction coefficient is the precondition based on the principle of drag reduction and drag reduction, , improving the dynamic and static friction conditions and improving the ability of the drilling tool system. AGBAJI[6] further studies the catenary track. It is pointed out that the quasi catenary can improve the position of the tilting point and reduce the slope.

This article draws on the previous research results of hydraulic pressurizer, combined with the installation of on-site pipe connection (shown in Figure 1). This paper provides a new basis for the design of the nozzle structure of hydraulic pressurizer by using CFD software to simulate the three-dimensional flow of the flow field near the nozzle of hydraulic pressurizer under different speeds and pressures.

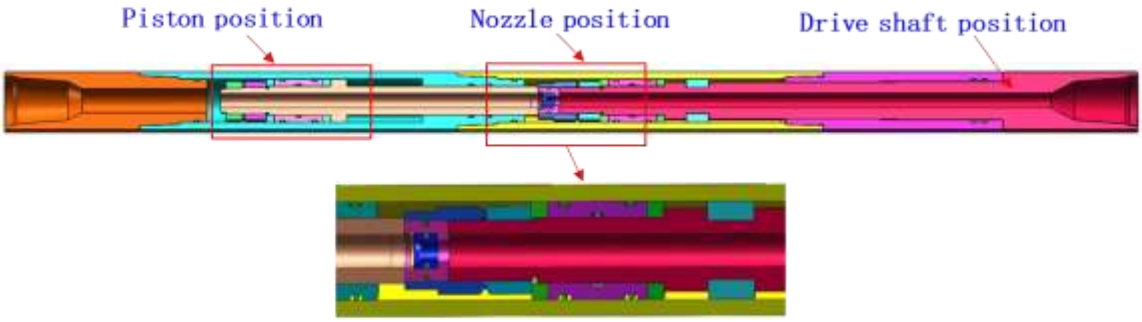

Figure 1: The whole and partial enlarged drawing of hydraulic thruster

2. Computational fluid dynamics controlling equations

The flow of fluids is controlled by the laws of conservation of mass, momentum, and energy, if the flow is in a turbulent state, the system also follows the additional turbulent transport equation, the control equation is a mathematical description of these conservation laws, the mathematical description of the physical model of the flow problem is given, that is the basic equation of flow (control equation) and its boundary conditions are given, which is known as mathematical model. The establishment of mathematical model is based on the physical model, in the study of hydraulic thruster, the geometry of the internal fluid region of hydraulic thruster is modeled by a three-dimensional solid model, flow state is in turbulent flow. Therefore, the mathematical model obtained is as follows [7, 8]:

1）Mass conservation equation

$$\frac{\partial \rho}{\partial t}+\frac{\partial}{\partial x}(\rho v_x)+\frac{\partial}{\partial r}(\rho v_r)+\frac{\rho v_r}{\partial r}=0 \quad (1)$$

2）Momentum conservation equation

$$\frac{\partial(\rho u_i)}{\partial t}+\frac{\partial(\rho u_i u_j)}{\partial x_i}=-\frac{\partial p}{\partial x_i}+\frac{\partial}{\partial x_i}(\eta\frac{\partial u_i}{\partial x_j}-\rho u_i{}' u_j{}') \quad (2)$$

3）energy-balance equation

$$\frac{\partial}{\partial t}(\rho T)+\frac{\partial}{\partial x}(\rho v_x T)+\frac{\partial}{\partial y}(\rho v_r T)=\frac{\partial}{\partial x}(\frac{k}{c_p}\frac{\partial T}{\partial x})+\frac{\partial}{\partial y}(\frac{k}{c_p}\frac{\partial T}{\partial y})+S_r \quad (3)$$

Where c_p is the specific heat capacity, This the temperature, K is the fluid heat transfer coefficient, S_r is the internal heat source of fluid and mechanical energy of fluid is converted into heat energy by viscous action, also it is known as viscous dissipation phase.

3. Flow field model establishment

In view of the feasibility of the actual numerical simulation of the flow field, the finite element modeling of the fluid near the nozzle of the hydraulic pressurizer, including the modeling of the upper and lower ends of the central pipe and the position of the nozzle and the refinement of the grid, is described in view of the flow field model, as shown in Figure 2.

Figure 2: Three-dimensional finite element model of flow field of hydraulic thruster

4. Determination of boundary conditions

4.1 Calculability Assumption

In the simulation study of the flow field of hydraulic pressurizer, the medium flowing through the center pipe of the hydraulic pressurizer is drilling fluid. In the process of flow, the density of working fluid varies greatly, so it treats it as a compressible fluid. At the same time, in the flow study, it is assumed that there is no leakage of fluid in the whole transmission process, that is, the law of conservation of mass; at the same time, there is no heat exchange between the hydraulic pressurizer and the surrounding environment, and the heat dissipation is also inside the hydraulic pressurizer: the principle of conservation of energy is observed. Because the whole flow path is basically in the same gravitational potential energy, it does not consider the influence of gravity (Gravitational forces), that is, ignoring the gravity term [9].

4.2 Boundary condition

Setting of boundary conditions: the outlet boundary condition is pressure outlet when the flow rate is 10, 12, 14 and 16L/s respectively in the main flow path. The drilling fluid density is 1.25kg/L, the inlet flow rate is set to 10, 12, 14 and 16L/s respectively, and the outlet pressure is 25MPa, as follows. Figure 3 shows that there is no slip solid wall condition on the wall of the nozzle and central pipe, which is $V_{wall}=0$, $W_{wall}=0$, $k_{wall}=0$, $\varepsilon_{wall}=0$.

Figure 3: Inlet and outlet boundary of flow field of hydraulic pressurizer

5. Calculation results analysis

5.1 Analysis of the result of flow field calculation

When flow rate Q=10L/s, flow field CFD finite element simulation calculation, get the whole velocity vector diagram of flow field model and pressure contour. As shown in Figure 4, from velocity vector diagram and profile contour, it is found that the velocity of the whole fluid varies from 0~56.987m/s. The erosion area is mainly located near the flow area of the nozzle, and the maximum erosion speed is 56.987m/s. It is found that the pressure gradually decreases from the inlet to the outlet. The pressure varies from 23.76MPa~25.6MPa to the nozzle, and the pressure gradually becomes smaller from the entrance to the nozzle, and then the nozzle to the outlet gradually becomes larger, and the pressure of the nozzle is minimal.

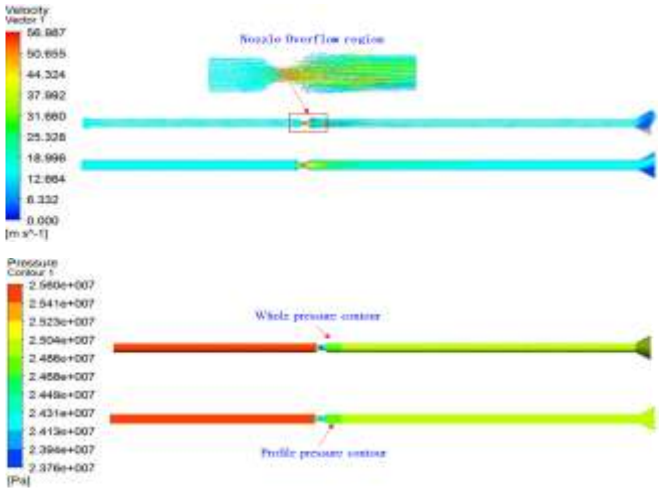

Figure 4: The whole velocity vector diagram and the pressure contour When Q=10L/s

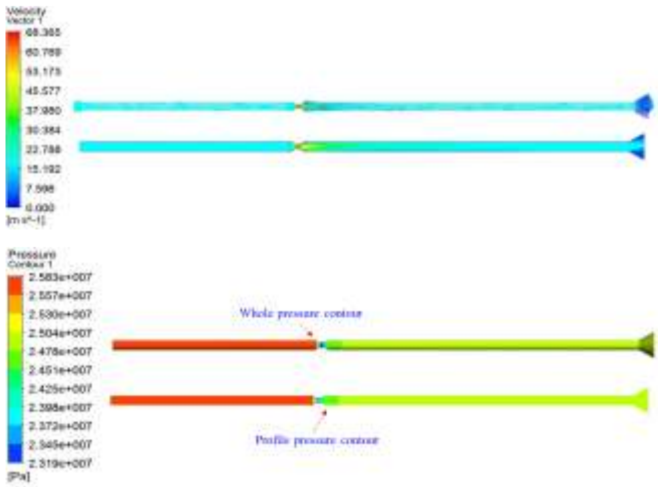

Figure 5: The whole velocity vector diagram and the pressure contour When Q=12L/s

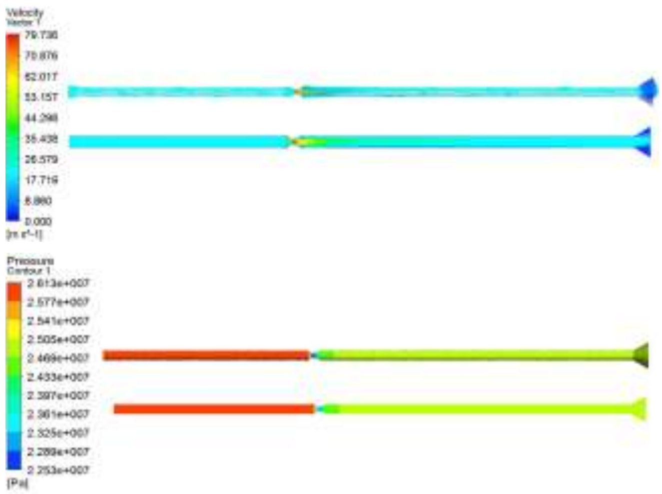

Figure 6: The whole velocity vector diagram and the pressure contour When Q=14L/s

International Journal of Science and Research (IJSR)
ISSN (Online): 2319-7064
Index Copernicus Value (2016): 79.57 | Impact Factor (2017): 7.296

When the flow rate is Q=12L/s, Q=14L/s and Q=16L/s, As shown in Figure 5, the velocity vector diagram and the profile cloud chart show that the velocity of the whole fluid varies from 0~68.365m/s to the nozzle, and the velocity is gradually increased from the inlet to the nozzle. It gradually decreases from the nozzle to the outlet. It is found that the pressure gradually decreases from the inlet to the outlet. The pressure varies from 23.19MPa~25.83MPa to the nozzle.

When the flow rate is Q=14L/s, as shown in Figure 6, the velocity of the whole fluid varies from 0~79.736m/s, and it is found that the pressure gradually decreases from the inlet to the outlet, and changes from the 22.53MPa~26.13MPa. When the flow rate is Q=16L/s, as shown in Figure 7, the velocity of the whole fluid varies from 0~91.103m/s. It is found that the pressure varies from the inlet to the outlet from the 21.8MPa~26.51MPa, and the pressure gradually becomes smaller from the inlet to the nozzle, and then the nozzle to the outlet gradually becomes larger, and the pressure in the nozzle is the least.

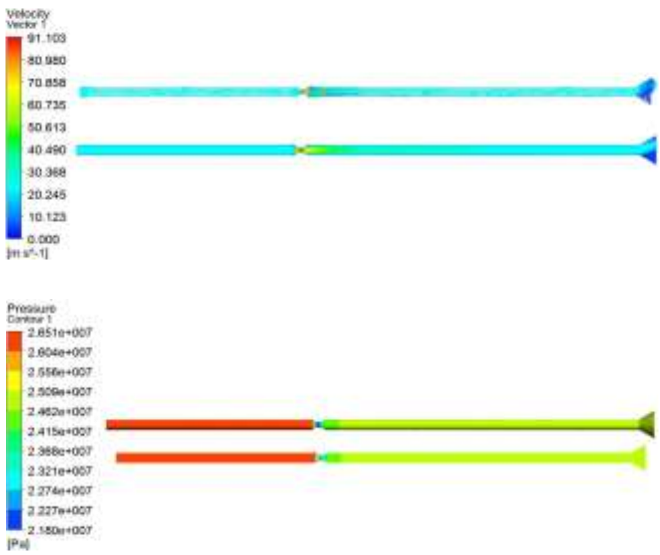

Figure 7: The whole velocity vector diagram and the pressure contour When Q=16L/s

5.2 Analysis of the curve of velocity and pressure

Figure 8 is a velocity graph on the main path of the fluid. It is found that the velocity of the main manifold varies from 60~90m/s to speed, and the velocity decreases from exit to inlet. As the flow rate increases, the overall velocity and maximum speed gradually become larger. When the flow rate is certain, the velocity has a stable period, and then the peak velocity near the nozzle, after the nozzle, the velocity becomes smaller, and then a stable range is reached.

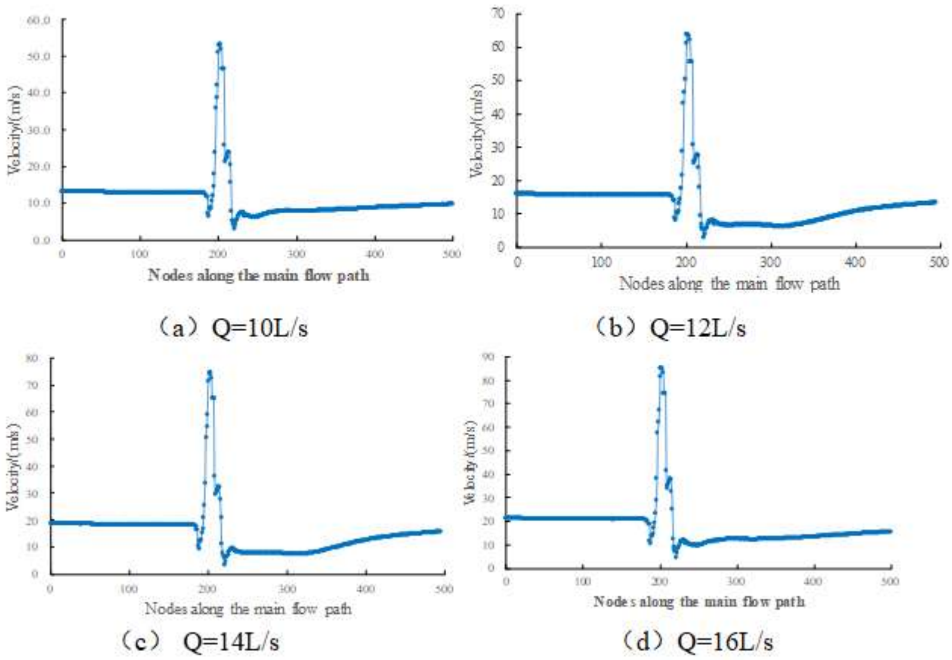

Figure 8: Fluid velocity curve on the main path under different flow rates

Figure 9 shows the fluid pressure curve on the main path of the main flow under different flow. It is found that the outlet of the fluid pressure of the pipe is gradually increased from the 25.5MPa~26.5MPa. With the flow increasing, the pressure has a stable period, and then the minimum pressure near the nozzle, after the nozzle, the pressure becomes smaller. After that, a stable range is reached.

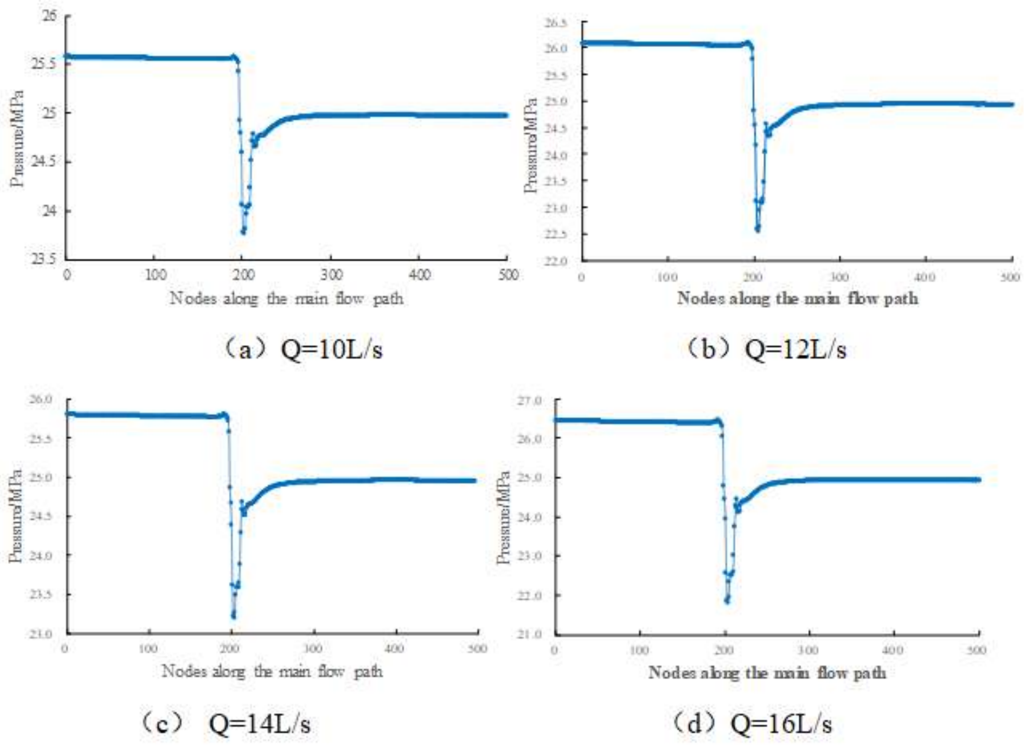

Figure 9: Fluid pressure curve on the main path under different flow rates

6. Conclusions

From the point of view of fluid mechanics, using the software of simulation analysis, we can get the following conclusions:

(1) The velocity vector diagram and the pressure cloud map of the flow field model, and the velocity gradually increases from the inlet to the nozzle, and then gradually decreases from the nozzle to the outlet. The erosion area is mainly located near the flow area of the nozzle. The maximum erosion speed is in the flow part of the nozzle. The pressure gradually decreases from the inlet to the outlet. The pressure is gradually reduced from the inlet to the nozzle, and then the nozzle to the outlet gradually becomes larger, and the pressure of the nozzle is minimal.

(2) It is found that the fluid velocity of the supervisor varies from 60~90m/s to speed, and the velocity decreases from exit to entrance. As the flow rate increases, the overall velocity and maximum speed gradually become larger. When the flow rate is certain, the velocity has a stable period, and then the peak velocity near the nozzle, after the nozzle, the velocity becomes smaller, and then a stable range is reached.

(3) The fluid pressure curve on the main path under different flow, the flow pressure of the main channel gradually becomes larger from the entrance to the exit, and changes from the 25.5MPa~26.5MPa. As the flow increases, the pressure has a stable period, and then the minimum pressure near the nozzle, after the nozzle, the pressure becomes smaller and then reaches the pressure. To a stable range.

Reference

[1] Lin Yuan hua, Huang Wan zhi, Shi Tai he. Wob calculation for combination of hydraulic thruster and downhole motor [J]. OIL DRILLING & PRODUCTION TECHNOLOGY, 1999, 21(1):20-23.
[2] Liu Jianming, Wei Xuecheng. Application of

hydraulic pressurizer in drilling of high steep structure in Northeast Sichuan [J]. Journal of Sheng li College China University of Petroleum, 2007, 21(2):8-11.

[3] Liu Qinzhi, Li Xingjie, Zhang Guotian, et al. Development and Field Application of Hydraulic Thruster [J]. CHINA PETROLEUM MACHINERY, 2013, 41(1):20-23.

[4] Tan Chunfei, Yu Liwei, Zhang Renlong, et al. Structural Design of the Hydraulic Thruster for Coiled Tubing Drilling [J]. CHINA PETROLEUM MACHINERY, 2012, 40(11):18-22.

[5] JOHN EM, TZUFANG C. The practice and evolution of torque and drag reduction: theory and field results [J]. SPE Annual Technical Conference and Exhibition, Denver, October 30-31, 2011[C]. USA: SPE, 2011.

[6] AGBAJI, ARMSTRONG L, et al. Optimizing the planning, design and drilling of extended reach and complex wells [J]. Abu Dhabi International Petroleum Conference, Abu Dhabi, November 1-4, 2010[C]. UAE, 2010.

[7] Zhang Mingyuan, Jing Sirui, Li Guojun. Advanced Engineering Fluid dynamics [M]. Xi 'an: xi 'an jiaotong university press, 2006.

[8] Hu Kun, Li Zhenbei. Detailed solution of engineering examples of ANSYS ICEM CFD [M]. Beijing: people post and Telecommunications Press, 2014.

[9] Zhang Shichao. Numerical Simulation and Analysis on Flow Field of Large Diameter Ball Valve Based on the CFD [J]. Mechanical research and Application, 2017, 30(1): 95–97